Cell and Tissue Research (2023) 392:167–178
https://doi.org/10.1007/s00441-022-03676-z

REVIEW

Prion strains viewed through the lens of cryo-EM

Szymon W. Manka[1] · Adam Wenborn[1] · John Collinge[1] · Jonathan D. F. Wadsworth[1]

Received: 28 May 2022 / Accepted: 18 August 2022 / Published online: 27 August 2022

Abstract
Mammalian prions are lethal transmissible pathogens that cause fatal neurodegenerative diseases in humans and animals. They consist of fibrils of misfolded, host-encoded prion protein (PrP) which propagate through templated protein polymerisation. Prion strains produce distinct clinicopathological phenotypes in the same host and appear to be encoded by distinct misfolded PrP conformations and assembly states. Despite fundamental advances in our understanding of prion biology, key knowledge gaps remain. These include precise delineation of prion replication mechanisms, detailed explanation of the molecular basis of prion strains and inter-species transmission barriers, and the structural definition of neurotoxic PrP species. Central to addressing these questions is the determination of prion structure. While high-resolution definition of ex vivo prion fibrils once seemed unlikely, recent advances in cryo-electron microscopy (cryo-EM) and computational methods for 3D reconstruction of amyloids have now made this possible. Recently, near-atomic resolution structures of highly infectious, ex vivo prion fibrils from hamster 263K and mouse RML prion strains were reported. The fibrils have a comparable parallel in-register intermolecular β-sheet (PIRIBS) architecture that now provides a structural foundation for understanding prion strain diversity in mammals. Here, we review these new findings and discuss directions for future research.

Keywords Cryo-EM · Prion · Prion disease · Prion strains · Prion structure

Introduction

Prions are exceptional lethal pathogens that cause fatal neurodegenerative diseases in mammals. These diseases include Creutzfeldt–Jakob disease (CJD), variant CJD (vCJD), kuru, fatal familial insomnia (FFI), and Gerstmann–Sträussler–Scheinker disease (GSS) in humans, and in animals, bovine spongiform encephalopathy (BSE) in cattle, scrapie in sheep and goats, and chronic wasting disease (CWD) in cervids (Prusiner 1998; Collinge 2001, 2005; Wadsworth and Collinge 2011; Greenlee and Greenlee 2015; Kim et al. 2017; Benestad and Telling 2018). Prions consist of infectious multichain fibrillar assemblies of misfolded host-encoded prion protein (PrP), a glycosylphosphatidylinositol (GPI)-anchored cell surface glycoprotein containing two asparagine (N)-linked glycosylation sites (Prusiner 1998; Wuthrich and Riek 2001; Collinge and Clarke 2007; Collinge 2016; Rodriguez et al. 2017). Prion propagation occurs by means of seeded protein polymerisation, involving recruitment of PrP monomers to existing fibrillar assemblies which elongate and then fragment to generate more "seeds" (Prusiner 1998; Collinge and Clarke 2007; Collinge 2016; Rodriguez et al. 2017; Meisl et al. 2021). Different prion strains produce different disease phenotypes in the same host and appear to be encoded by fibrillar assemblies with distinct misfolded PrP conformations and PrP glycoform assembly states (Collinge et al. 1996; Prusiner 1998; Collinge and Clarke 2007; Wadsworth et al. 2010; Wadsworth and Collinge 2011; Collinge 2016).

While historically rare in humans, the appearance of vCJD in the UK from 1995 onwards (Will et al. 1996; Collinge et al. 1996; Collinge 1999), and the experimental confirmation that this was caused by dietary exposure to BSE prions from cattle (Collinge et al. 1996; Hill et al. 1997; Bruce et al. 1997; Asante et al. 2002), spurred intense international efforts to understand the fundamental basis of prion transmission barriers in order to protect public health (Collinge 1999, 2001; Wadsworth

✉ John Collinge
jc@prion.ucl.ac.uk

✉ Jonathan D. F. Wadsworth
j.wadsworth@prion.ucl.ac.uk

[1] MRC Prion Unit at UCL, Institute of Prion Diseases, University College London, 33 Cleveland Street, London W1W 7FF, UK

and Collinge 2011). While public and animal health controls to limit human exposure to BSE prions have been highly effective, the existence or emergence of other animal prion strains with zoonotic potential is of considerable concern. In particular, CWD is a contagious disease in free-ranging and captive cervid populations and considerable human exposure may be occurring in North America through consumption of hunted deer (Benestad and Telling 2018; Escobar et al. 2020; Tranulis et al. 2021). In 2016, CWD was also reported in Europe (Benestad and Telling 2018; Tranulis et al. 2021). As it is well known that novel, potentially zoonotic, prion strains with altered host ranges can arise as a result of PrP polymorphisms in both inter- and intra-species transmissions (Collinge and Clarke 2007; Wadsworth et al. 2010; Wadsworth and Collinge 2011; Collinge 2016; Moreno and Telling 2017; Mead et al. 2019), understanding how prion strains are encoded is of high importance (Watson et al. 2021).

PrP monomer incorporation into infectious, protease-resistant, detergent-insoluble fibrillar prion assemblies (classically designated as PrP^{Sc} (Prusiner 1998)) requires gross rearrangement of the protein fold (Fig. 1). While the cellular isoform of PrP (PrP^{C}) has globular C-terminal domain containing three α-helices (Wuthrich and Riek 2001; Rodriguez et al. 2017) (Fig. 1a, b), and is soluble in detergents and readily digested by proteases, PrP monomers within detergent-insoluble, infectious PrP^{Sc} fibrils adopt a β-strand-rich configuration (Pan et al. 1993; Prusiner 1998) that confers protease-resistance to the C-terminal two-thirds of the PrP polypeptide (Meyer et al. 1986; Prusiner 1998; Wenborn et al. 2015; Kraus et al. 2021; Manka et al. 2022b; Hoyt et al. 2022) (Fig. 1a and c, d). Proteinase K (PK)-digestion of PrP^{Sc} generates a classical PrP 27–30 banding pattern on SDS-PAGE gels/western blots, comprising C-terminal proteolytic fragments of di-, mono-, and non-glycosylated PrP (Meyer et al. 1986; Prusiner 1998; Wenborn et al. 2015; Kraus et al. 2021; Manka et al. 2022b; Hoyt et al. 2022). The overall similarity of PrP 27–30 banding patterns seen across multiple human and animal prion strains is indicative of a generic fibrillar prion architecture. However, strain-specific signatures of proteolytic fragment sizes and PrP glycoform ratios indicate structural variation in fibrils of different strains (Bessen and Marsh 1994; Telling et al. 1996; Collinge et al. 1996; Parchi et al. 1999; Safar et al. 1998; Hill et al. 2003; Wadsworth et al. 2004; Hill et al. 2006; Wadsworth and Collinge 2011; Wenborn et al. 2015).

The detailed arrangement of β-strands and overall architecture of infectious ex vivo prion fibrils (also referred to as prion rods (Prusiner et al. 1983; Prusiner 1998; Terry and Wadsworth 2019)) have been intensely debated, reviewed by Rodriguez et al. (2017), Baskakov et al. (2019), and Terry and Wadsworth (2019). Two major structural models have been proposed, the parallel in-register intermolecular β-sheet (PIRIBS) architectures (Groveman et al. 2014; Artikis et al. 2020) and a 4-rung beta solenoid model (Vazquez-Fernandez et al. 2016; Spagnolli et al. 2019). While PrP amyloids formed in vitro from recombinant PrP have PIRIBS architectures (Cobb et al. 2007; Tycko et al. 2010; Groveman et al. 2014; Theint et al. 2017; Wang et al. 2020, 2021; Glynn et al. 2020) (Fig. 2a, c), such assemblies are either devoid of detectable prion infectivity or have such low specific-infectivity that observed structures cannot be reliably correlated with biological activity (Collinge and Clarke 2007; Schmidt et al. 2015; Collinge 2016; Terry and Wadsworth 2019). Efforts to elucidate authentic prion structures have therefore remained reliant upon structural characterisation of ex vivo purified material of high specific infectivity and in a form suitable for structural study.

Fig. 1 Prion protein conversion into infectious prion fibrils. **a**, **b** ▶ Atomistic model of mature mouse PrP^{C} (residues 23–230), including post-translational modifications (carbohydrate groups, pink; sialic acid groups, red), anchored in the phospholipid bilayer (coloured by heteroatom: C, white; P, orange; N, blue; O, red). Proteinase K (PK)-sensitive region (residues 23–89, light grey) refers to PK-sensitivity after conversion to prion fibrils (see panel **d**). The model was built in CHARMM-GUI (https://www.charmm-gui.org/) (Jo et al. 2008) and UCSF Chimera (Pettersen et al. 2004), using a solution NMR structure of the GPI-anchor from human complement regulatory protein CD59 (pdb ID: 1CDR) (Fletcher et al. 1994), an X-ray structure of the mouse PrP (pdb ID: 4H88) (Sonati et al. 2013), and X-ray structures of tri-antennary N-linked sialylated glycans from human prostate specific antigen glycoprotein (pdb ID: 3QUM) (Stura et al. 2011). The close-up view (**b**) shows the portion of the PrP^{C} chain (ribbon representation) that contributes specific sub-domains in PrP^{Sc}, as indicated with distinct colours. Selected secondary structures are labelled. **c** Mouse PrP sequence with colour-coded prion fibril PrP^{Sc} sub-domain ranges. PK-resistant RML fibril core (panel **d**, top; residues 89–230) includes amyloid core (residues 94–225; grey highlight). N180 and N196 glycosylation sites are numbered in red. **d** RML (pdb ID: 7QIG) (Manka et al. 2022b) and 263K (pdb ID: 7LNA) (Kraus et al. 2021) PrP^{Sc} fibril structures (3 subunits, ribbon representation) coloured as in (**a**–**b**). N- and C-terminal flexible tails (residues 89/90–93/94 and 226/227–230/231, mouse/hamster numbering) have been added to the models, together with post-translational modifications. The 263K model has additional residues 94–96 modelled at the tips of the C-terminal lobe hairpins, due to their absence in the original structure. Major internal hydrophobic clusters that contribute to fold stability (1–6) are shown with surface representation. Mouse-to-hamster substitutions in PrP sequence are indicated in the 263K structure (hamster numbering). S–S, disulphide bond

Progress with purifying prions

Purification of prions from mammalian brain is highly challenging due to their low abundance in affected tissue and the requirement to maintain and measure biological activity throughout purification. The seminal purification procedures developed by Prusiner and colleagues (Bolton et al. 1982; McKinley et al. 1983; Prusiner et al. 1983, 1987; Bolton and Bendheim 1991) were a remarkable accomplishment and led

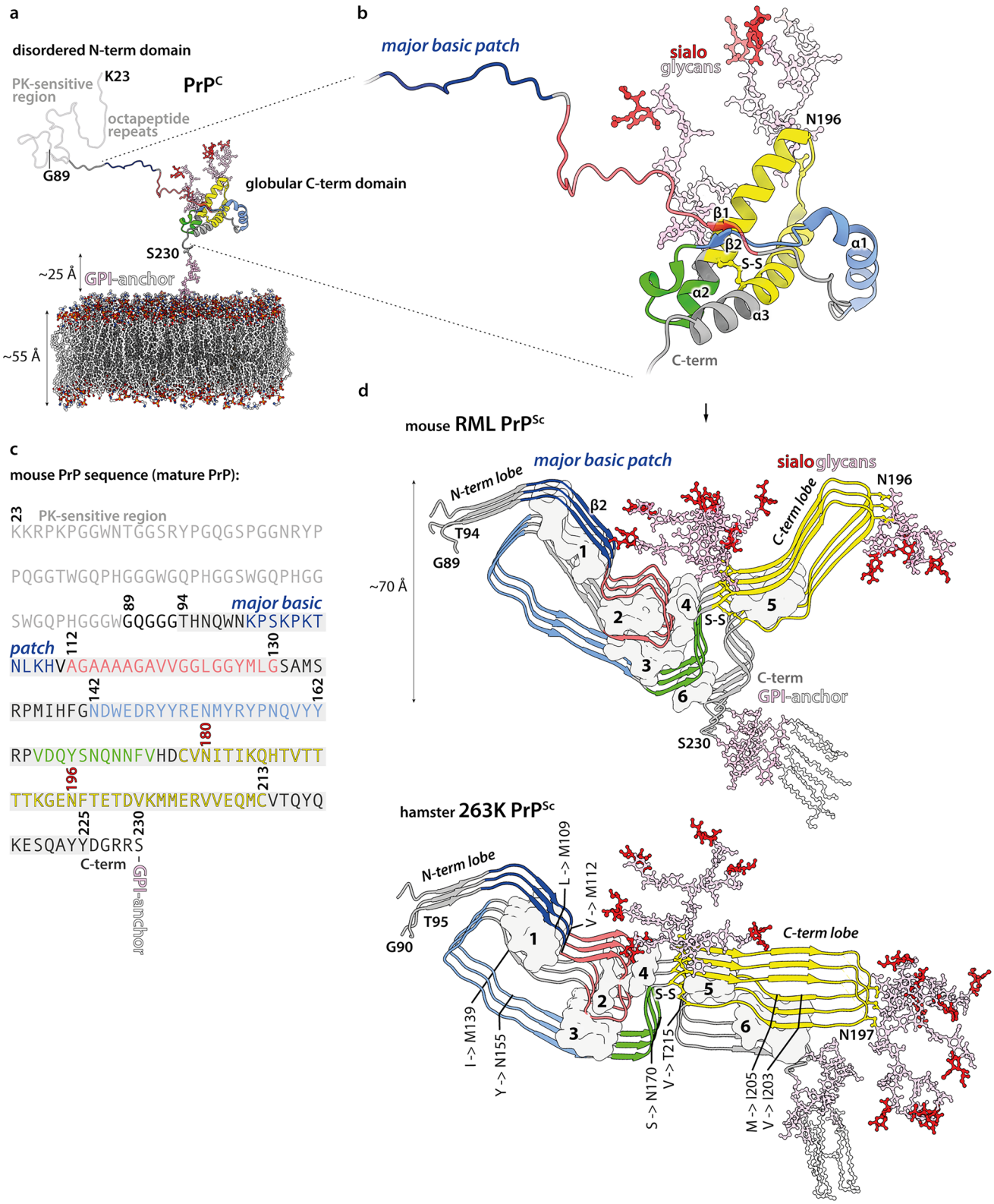

to the discovery of infectious prion rods (Prusiner et al. 1983). However, the complexity of these procedures and the requirement for large quantities of infected brain has precluded their widespread application and progress with developing alternative purification strategies has been impeded by an historical reliance on rodent bioassay.

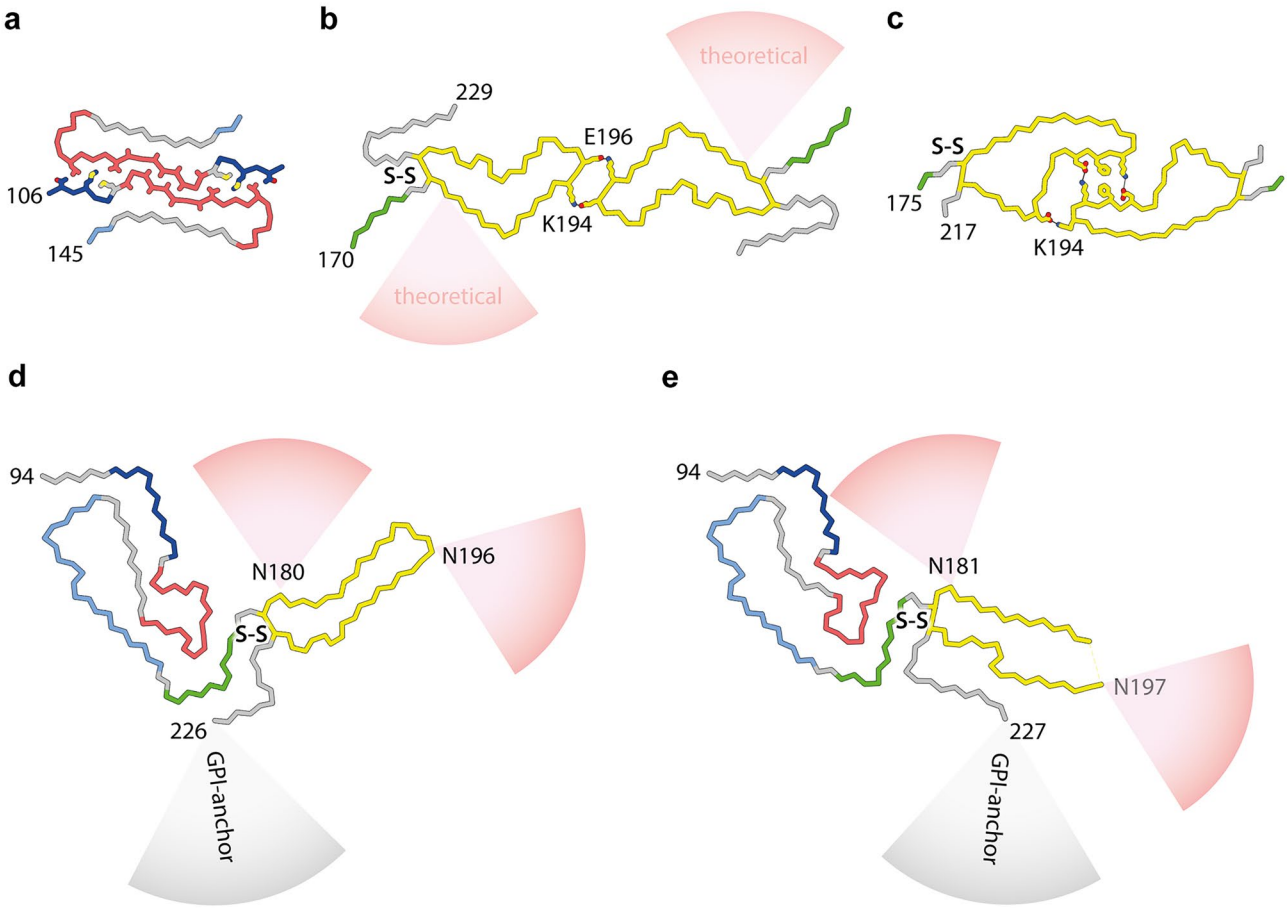

Fig. 2 PrP chain conformations in recombinant and ex vivo PrP fibrils **a**–**c** PrP folds and protofilament pairing interfaces in fibrils grown in vitro from recombinantly expressed PrP substrates (human sequence): **a** 106–145 9.7 kDa fragment (M129 variant) (Glynn et al. 2020); **b** 23–231 (full-length) PrP (Wang et al. 2020) with schematically indicated theoretical sialoglycan occupancy (red cones), as modelled by Artikis et al. (2020); **c** full-length PrP with familial prion disease-related mutation E196K (Wang et al. 2021). **d** RML protofibril (Manka et al. 2022b). **e** 263K protofibril (Kraus et al. 2021). Structures in all panels (**a**–**e**) represent fibril cores with species-specific numbering of start and end residues. PrP subunits are shown predominantly as backbones coloured according to ex vivo fibril sub-domain assignment defined in Fig. 1. Residues involved in PrP protofibril pairing (contributing to experimentally confirmed inter-protofilament interfaces) are shown with side chains coloured by heteroatom (N, blue; O, red; S, yellow; C, as backbone) and salt bridges or hydrogen bonds stabilising the two-protofilament architecture are indicated with black lines. Selected interfacing and glycosylated residues are labelled. S–S, disulphide bond

The availability of cell-based prion bioassays (Klohn et al. 2003; Mahal et al. 2007) and their automation (Schmidt et al. 2015) has provided the opportunity to explore the development of alternative prion purification strategies. Using the scrapie cell assay (Klohn et al. 2003) to track prion infectivity, we developed novel and simplified procedures for isolating extremely pure, high-titre intact infectious prion rods from small quantities of brain tissue from different hosts (Wenborn et al. 2015). Levels of purity of these samples are comparable with those generated using the best historical protocols, and importantly, as no specialised materials or equipment are required, the method is accessible to most existing prion laboratories. Purified prion rods produced by these methods constitute the authentic infectious prion assembly state as they can be physically correlated with infectivity by bioassay of electron microscopy grids or atomic force microscopy mica supports in cell culture (Terry et al. 2016, 2019) and faithfully transmit prion strain-specific phenotypes when inoculated into mice (Wenborn et al. 2015). These data firmly establish purified prion rods as the target for high-resolution structural investigation of prion strains.

Progress in cryo-EM and amyloid 3D structure determination

Advances in cryo-EM (Bai et al. 2015; Henderson 2018; Frank 2018; Dubochet 2018; Saibil 2022) and image processing in Relion (He and Scheres 2017; Zivanov et al. 2018;

Scheres 2020; Kimanius et al. 2021; Lövestam and Scheres 2022) have enabled direct, high-resolution structural studies of amyloids, fibrillar polymers defined by cross-β structure, in which misfolded protein monomers stack to form a ribbon of intermolecular β-sheets (Eisenberg and Sawaya 2017; Rodriguez et al. 2017; Fitzpatrick and Saibil 2019; Gallardo et al. 2020; Sawaya et al. 2021). In a series of seminal studies using purified fractions from human brains, cryo-EM and image processing in Relion revealed the structures of diverse self-propagating assemblies of tau (Fitzpatrick et al. 2017; Falcon et al. 2018, 2019; Zhang et al. 2020; Shi et al. 2021), amyloid-β (Kollmer et al. 2019; Ghosh et al. 2021; Yang et al. 2022a), and α-synuclein (Schweighauser et al. 2020; Yang et al. 2022b). These remarkable methods and data now lay the foundation for structure-based classification of the commoner neurodegenerative diseases and exploration of the general applicability of prion-like propagation and the strain phenomenon in determining phenotype (Shi et al. 2021; Sawaya et al. 2021; Kovacs et al. 2022).

Recent cryo-EM structures of ex vivo hamster 263K and mouse RML prion fibrils

High-resolution cryo-EM studies of infectious, brain-derived, prion samples isolated from the hamster 263K prion strain (Kraus et al. 2021) or the mouse RML prion strain (Manka et al. 2022b) discovered single-protofilament, left-handed helical PIRIBS amyloid fibrils that have a remarkably similar overall architecture, despite eight mouse vs. hamster amino acid substitutions (Fig. 1d). In both protofibrils, a single PrP subunit folds to create distinct N- and C-terminal lobes that form each protease-resistant rung of the fibril with protease-resistant cores that correspond to the sequences expected from the strain-specific signature PrP 27–30 truncated PrP^{Sc} banding patterns seen on western blots. GPI-anchorless PrP transgenic mice infected with wild-type RML prions propagate poorly glycosylated prion fibrils (designated aRML) whose fold is very similar to wild-type RML fibrils (Hoyt et al. 2022; Manka et al. 2022b). These findings establish that the wild-type RML fibril fold can be stably propagated utilising mouse PrP lacking post-translational modifications (Hoyt et al. 2022; Manka et al. 2022b).

The N-terminal lobe exhibits more conformational similarity between the 263K and RML strains than the C-terminal lobe that harbours the two N-linked glycans and the GPI anchor (Fig. 1d). Besides the typical longitudinal (inter-chain) cross-β hydrogen bonds in the PIRIBS arrangement, the folds are also stabilised by lateral inter- and intra-chain polar interactions and by six major hydrophobic clusters internal to the fold. These hydrophobic clusters provide both lateral and longitudinal stabilisation to the assembly (Fig. 1d). The overall positions of clusters 1–5 are similar between the two strains; however, cluster 6 is formed by different residues due to divergent C-terminus configuration in each strain (Fig. 1d). This change in C-terminus position likely results from mouse vs. hamster differences in PrP primary structure that map to both (alternative) locations of cluster 6 (Fig. 1d, bottom panel). It also results in the GPI-anchor being much closer to the second (N197) glycosylation site in the 263K fibril, compared to RML fibril (Fig. 1d).

The N- and C-terminal lobes can be further sub-divided into common motifs and folding modules. The first two are the major basic patch (residues 100/101–110/111, mouse/hamster sequence) and the low-complexity Gly/Ala-rich region (residues 112/113–130/131, mouse/hamster sequence), formed from the disordered N-terminal part of PrP^{C} (Fig. 1b and d). The major basic patch (comprising the second β-sheet) shows a relatively conserved topology between the two strains despite two amino acid substitutions, whereas the sequence-wise conserved Gly/Ala-rich region adopts a unique fold in each strain (Fig. 1d).

The major basic patch seems to be firmly stabilised by hydrophobic cluster 1 in both strains (Fig. 1d). Strikingly, the cluster itself is conserved in the two rodent species albeit with three hydrophobic amino acid substitutions (Fig. 1d). In the hamster PrP sequence the L108, V111 and I138 residues (mouse numbering) are replaced with the methionine triad (M109, M112, and M139, hamster numbering) (Kraus et al. 2021; Manka et al. 2022b). The relatively long, inwardly pointed Met side chains (Kraus et al. 2021) considerably widen the respective β-hairpin structure (Fig. 1d). Notably, a single M for I substitution at the position 138 (mouse numbering) was found to be inhibitory for scrapie prion propagation in mouse neuroblastoma cells in 1995 (Priola and Chesebro 1995). Now, after 27 years, we can appreciate how this single amino acid mismatch may cause a prion transmission barrier, at least in this particular cell-based system.

Hydrophobic clusters 2 and 3 stabilise variable conformations of the low-complexity Gly/Ala-rich region within the N-terminal lobe, whereas hydrophobic cluster 4 provides this region with additional hydrophobic anchorage at the inter-lobe interface in both protofibrils (Fig. 1d). On the other side of the N-terminal lobe, the sequence 142/143–162/163 (mouse/hamster numbering) (which in PrP^{C} forms the first α-helix (α1), the second (short) β-strand (β2) and the intervening α1-β2 loop (Fig. 1b)) shows a similarly folded region in both fibril structures (Fig. 1b and d). It is almost immediately followed by the sequence 165/166–175/176 (mouse/hamster numbering), which in PrP^{C} comprises the β2-α2 loop (Fig. 1b), that folds to create the C-terminal side of the inter-lobe interface and interacts with the Gly/Ala-rich region in both fibrils (Fig. 1b and d).

The disulphide-stapled hairpin is a major part of the C-terminal lobe in both strains and shows a distinct conformation in each strain, which requires unravelling α-helices 2 and 3 of PrP^C. Unlike the RML disulphide-stapled hairpin, the 263K hairpin widens towards its tip, presumably due to the unique, hydrophobic cluster 6-mediated interaction with the C-terminus, as described above (Fig. 1d). This 263K-specific interaction may also be responsible for widening of the cleft between the N- and C-terminal lobes in the 263K fibril compared to the RML fibril, which potentially reduces spatial constraints for the N180-glycan in the former compared to the latter (Figs. 1d and 2d, e).

Overall, the PIRIBS structure of the three ex vivo prion fibrils characterised to date (Kraus et al. 2021; Manka et al. 2022b; Hoyt et al. 2022) is compatible with earlier studies that examined ex vivo material using a variety of other techniques (reviewed in Kraus et al. (2021)) and with the defining physicochemical properties of prions (Kraus et al. 2021; Manka et al. 2022b; Hoyt et al. 2022). These authentic infectious prion fibrils appear to incorporate particularly long polypeptide chains into their amyloid cores compared to the other disease-related amyloids that have been characterised so far (Sawaya et al. 2021; and see The Amyloid Atlas https://srv.mbi.ucla.edu/AmyloidAtlas/), and such unique fibril structures, stabilised by cohorts of internal hydrophobic clusters spanning the entire length and width of the fibrils, may explain the exceptional stability of prions and their resistance to clearance by the host.

Cryo-EM structures of recombinant PrP fibrils

To date, no in vitro-generated fibrils polymerised from recombinant (anchorless and strictly non-glycosylated) PrP monomers have replicated the structures of ex vivo prion fibrils. All recombinant PrP fibrils so far characterised by cryo-EM consist of two symmetrical protofilaments with smaller amyloid cores than those of ex vivo infectious prion fibrils (Wang et al. 2020, 2021; Glynn et al. 2020) (Fig. 2). None of these structures have been reported to be infectious (Wang et al. 2020, 2021; Glynn et al. 2020).

Notably, the recombinant PrP fibrils show various geometries and pairing interfaces (Wang et al. 2020, 2021; Glynn et al. 2020) (Fig. 2a–c). Such pairing promiscuity appears to be only possible for the relatively small, non-glycosylated amyloid cores of recombinant PrP fibrils, as the observed pairing modes are largely incompatible with the ex vivo fibril folds or the locations of N-linked glycans (Fig. 2d, e).

Paired prion fibrils

Consistent with previous studies (Terry et al. 2016, 2019), our recent high-resolution cryo-EM studies showed that RML protofibrils can associate laterally, forming two-protofilament fibrils (Manka et al. 2022b) (Fig. 2d). However, analogous paired assemblies of 263K protofibrils were not reported (Kraus et al. 2021). The reason for this difference is currently unclear, and in this regard, we do not know how different prion extraction and purification protocols used in our work and that of Caughey and colleagues might influence protofilament pairing. Kraus et al. used high salt concentrations (1.7 M NaCl) (Kraus et al. 2021), and we used phosphotungstate (PTA) polyanions that clearly decorate RML fibrils along the major basic patch and in the vicinity of the inter-protofilament interface of the predominant paired fibril structure identified in our cryo-EM dataset (Manka et al. 2022b) (EMPIAR-10992). In the absence of a high-resolution 3D reconstruction, it cannot be excluded that PTA clusters are capable of bridging two RML protofibrils together or modulating existing paired fibril geometries. Indeed, more than one mode of RML protofibril pairing was detected in our cryo-EM dataset (Manka et al. 2022b) (EMPIAR-10992). However, crucially, we confirmed that pairing per se is independent of PTA, as paired protofilaments are also present in ex vivo RML prion preparations that excluded PTA (Manka et al. 2022b).

Potential mechanisms underlying prion-strain specific PrP glycoform ratios

Not all prion strains are considered to be PrP sialoglycoform-selective. The hamster 263K strain is an example of such non-selective strain, whose PrP sialoglycoform composition appears to reflect the natural (physiological) abundance of PrP^C sialoglycoforms, in which di-glycosylated PrP is dominant (Katorcha and Baskakov 2017). In contrast, the RML strain has diminished di- and enriched mono- and non-glycosylated PrP composition (Wenborn et al. 2015; Katorcha and Baskakov 2017; Kang et al. 2020; Manka et al. 2022b). Thus, the architecture of the RML prion is expected to sterically restrict incorporation of di-glycosylated PrP chains and favour incorporation of mono- and non-glycosylated PrP. On the basis of the existing data, it is not readily apparent how this could be achieved based solely on the single protofilament architecture. Indeed, in silico modelling suggests no obvious steric hindrance or energetic penalty for accommodating even large tri-antennary sialoglycans at every rung of the PIRIBS structure of a recombinant PrP fibril (Artikis et al. 2020) (shown in Fig. 2b). Paired assemblies of RML protofilaments, however, could confine the space

available for N-glycan incorporation (Manka et al. 2022b). Clearly further work on the paired assemblies is required and such future work may establish whether protofilament pairing is a specific property of glycoform selective strains or a universal phenomenon across prion strains.

Prions versus transmissible PrP amyloid

Human prion diseases are associated with a range of clinical presentations, and they are classified by both aetiology and clinicopathological syndrome, with subclassification according to molecular criteria (Collinge et al. 1996; Collinge 2001; Parchi et al. 1999; Hill et al. 2003; Wadsworth and Collinge 2011; Baiardi et al. 2018; Mead et al. 2019). Approximately 15% of cases are associated with autosomal dominant pathogenic mutations in the human prion protein gene (*PRNP*), and to date, more than sixty mutations have been described (Mead et al. 2019). These include insertions of between four and twelve extra repeats within the octapeptide repeat region (Fig. 1a) between codons 51 and 91, a two-octapeptide repeat deletion and various other mutations causing missense or stop substitutions or other insertions with and without a frameshift (Mead et al. 2019).

Pathogenic *PRNP* mutations appear to have diverse and direct effects on dictating the preferred structure or assembly state of mutant PrP prion assemblies and cases of inherited prion disease caused by point mutations have PrP 27–30 glycoform ratios distinct from those seen in both sporadic and acquired CJD human prion diseases (Piccardo et al. 1998; Parchi et al. 1998; Furukawa et al. 1998; Cardone et al. 1999; Hill et al. 2006). Moreover, in distinction to sporadic or acquired CJD, a common feature in patients with diverse *PRNP* point mutations is that the expressed full-length mutant PrP generates two distinct types of disease-related PrP assembly. One corresponds to authentic prions that generates classical PrP 27–30 patterns of N-terminally truncated PrP^{Sc} and is found in brain areas showing synaptic PrP deposition, spongiform vacuolation, and neurodegeneration. The other type of assembly forms smaller N- and C-terminally truncated protease-resistant fragments (typically 7–15 kDa, derived from the central region of PrP) and is associated with prominent PrP amyloid plaques that are commonly seen in some inherited prion diseases (Giaccone et al. 1992; Piccardo et al. 1996, 1998, 2001; Parchi et al. 1998; Salmona et al. 2003; Hill et al. 2006; Wadsworth et al. 2006; Monaco et al. 2012; Asante et al. 2013, 2020; Ghetti et al. 2018; Cracco et al. 2019). Variation in the PrP conformation of authentic prion fibrils and distinct PrP amyloids (governed by the specific PrP missense mutation) would be expected to dictate highly specific strain transmission properties via conformational selection (Collinge 1999, 2016; Collinge and Clarke 2007; Wadsworth et al. 2010) as has recently been demonstrated for *PRNP* P102L and A117V mutations (Asante et al. 2009, 2013, 2015, 2020).

Importantly, temporal and spatial differences in the propagation of authentic prions or alternative PrP amyloids within the brain may readily account for the wide diversity of clinicopathological phenotypes seen in family members with the same *PRNP* mutation (Parchi et al. 1998; Kovacs et al. 2002; Piccardo et al. 2007; Webb et al. 2008; Mead and Reilly 2015; Barron et al. 2016; Choi et al. 2016; Barron 2017; Kim et al. 2017; Ghetti et al. 2018; Mead et al. 2019; Asante et al. 2020) with further complexity contributed by variable involvement of pathological conformers of wild type PrP (Gabizon et al. 1996; Silvestrini et al. 1997; Chen et al. 1997; Wadsworth et al. 2006; Monaco et al. 2012). Notably, while patients with different *PRNP* missense mutations that produce full length mutant PrP can co-propagate authentic prions and alternative PrP amyloids, patients with *PRNP* stop mutations which produce C-terminally truncated PrP devoid of N-linked glycans and GPI-anchor (for example, Y145X (Ghetti et al. 1996) or Y163X (Mead et al. 2013)) may only propagate PrP amyloids giving rise to distinct disease phenotypes (Mead and Reilly 2015; Ghetti et al. 2018). To date, high-resolution structural studies of ex vivo prions and alternative PrP amyloids from human brain have been extremely problematic due to biosafety obstacles; however, very recently, cryo-EM structures of prion protein filaments from Gerstmann-Sträussler-Scheinker disease (F198S) have been reported (Hallinan et al. 2022).

Progress in defining the neurotoxic PrP species

Prion pathogenesis involves progressive loss of neuronal cells, and it has been long assumed that prions are directly neurotoxic. However, using a new multi-parametric assay of prion neurotoxicity in primary neurons, we recently examined exceptionally pure preparations of highly infectious, ex vivo RML prion fibrils devoid of contaminating proteins or small oligomeric PrP assemblies in cell culture alongside RML prion-infected mouse brain homogenates. Prion-infected brain homogenates were toxic as measured by neurite retraction and fragmentation and reduction in dendritic spine density (Benilova et al. 2020). In sharp contrast, highly purified infectious prion fibrils (100–200 nm in length) were not toxic and did not induce neurite retraction even when at prion titres much higher than that present in the infected brain homogenate (Benilova et al. 2020). Significantly, treatment of brain homogenate with the detergent sarkosyl abolished neurotoxicity, while infectivity was unaffected. These data clearly suggest that neurotoxicity is not attributable to infectious prion assemblies regardless of their aggregate size or

relative protease sensitivity (Benilova et al. 2020). The lack of detectable direct toxicity of highly purified prion preparations or sarkosyl-treated infected brain homogenate is consistent with models of prion neurotoxicity being mediated by a distinct oligomeric or monomeric PrP isoform designated PrP^{L} (for lethal) that may be generated by a distinct mechanistic process (Collinge and Clarke 2007; Sandberg et al. 2011, 2014; Collinge 2016; Benilova et al. 2020).

Concluding remarks

Undoubtedly, we have just entered a very exciting era for prion research, where methods for prion fibril purification and near-atomic structure determination by single particle cryo-EM are established (Telling 2022). A flurry of ex vivo prion fibril structures can now be expected (see for example Manka et al. (2022a)). Defining prion replication mechanisms responsible for maintaining the signature glycoform ratios of diverse prion strains remains a considerable research challenge, and it now seems clear that determining the relevance of paired fibril assemblies may be critical to achieving this. Understanding mechanisms of neurotoxicity in prion disease pathogenesis remains highly challenging; however, new neurotoxicity assays are now enabling systematic isolation of the neurotoxic PrP species that will facilitate detailed structural characterisation (Benilova et al. 2020). Future microscopy-based research is now also likely to move toward high-resolution studies of prion interactions with their cellular or extracellular binding partners and in this regard several extracellular matrix proteins or cell surface receptors have been implicated in prion pathogenesis (Moretto et al. 2022). Correlative light and electron cryotomography involving fluorescent labelling of PrP in a way that does not interfere with prion propagation will be necessary for facilitating this future research. This would then permit identification of relevant prion structures within the complex environments of cell cultures or tissue sections.

Funding This work was funded by the core award to the MRC Prion Unit at UCL from the UK Medical Research Council (MC_UU_00024/5).

Declarations

Ethical approval Not applicable.

Informed consent Not applicable.

Conflict of interests J. C. is a director and J. C. and J. D. F. W. are shareholders of D-Gen Limited, an academic spin-out company working in the field of prion disease diagnosis, decontamination, and therapeutics. S. W. M. and A. W. declare no competing interests.

References

Artikis E, Roy A, Verli H, Cordeiro Y, Caughey B (2020) Accommodation of in-register N-linked glycans on prion protein amyloid cores. ACS Chem Neurosci 11:4092–4097

Asante EA, Gowland I, Grimshaw A, Linehan JM, Smidak M, Houghton R, Osiguwa O, Tomlinson A, Joiner S, Brandner S, Wadsworth JD, Collinge J (2009) Absence of spontaneous disease and comparative prion susceptibility of transgenic mice expressing mutant human prion proteins. J Gen Virol 90:546–558

Asante EA, Grimshaw A, Smidak M, Jakubcova T, Tomlinson A, Jeelani A, Hamdan S, Powell C, Joiner S, Linehan JM, Brandner S, Wadsworth JD, Collinge J (2015) Transmission properties of human PrP 102L prions challenge the relevance of mouse models of GSS. PLoS Pathog 11:e1004953

Asante EA, Linehan J, Desbruslais M, Joiner S, Gowland I, Wood A, Welch J, Hill AF, Lloyd S, Wadsworth JD, Collinge J (2002) BSE prions propagate as either variant CJD-like or sporadic CJD-like prion strains in transgenic mice expressing human prion protein. EMBO J 21:6358–6366

Asante EA, Linehan JM, Smidak M, Tomlinson A, Grimshaw A, Jeelani A, Jakubcova T, Hamdan S, Powell C, Brandner S, Wadsworth JD, Collinge J (2013) Inherited prion disease A117V is not simply a proteinopathy but produces prions transmissible to transgenic mice expressing homologous prion protein. PLoS Pathog 9:e1003643

Asante EA, Linehan JM, Tomlinson A, Jakubcova T, Hamdan S, Grimshaw A, Smidak M, Jeelani A, Nihat A, Mead S, Brandner S, Wadsworth JDF, Collinge J (2020) Spontaneous generation of prions and transmissible PrP amyloid in a humanised transgenic mouse model of A117V GSS. PLoS Biol 18:e3000725

Bai XC, McMullan G, Scheres SH (2015) How cryo-EM is revolutionizing structural biology. Trends Biochem Sci 40:49–57

Baiardi S, Rossi M, Capellari S, Parchi P (2018) Recent advances in the histo-molecular pathology of human prion disease. Brain Pathol 29:278–300

Barron RM (2017) Infectious prions and proteinopathies. Prion 11:40–47

Barron RM, King D, Jeffrey M, McGovern G, Agarwal S, Gill AC, Piccardo P (2016) PrP aggregation can be seeded by pre-formed recombinant PrP amyloid fibrils without the replication of infectious prions. Acta Neuropathol 132:611–624

Baskakov IV, Caughey B, Requena JR, Sevillano AM, Surewicz WK, Wille H (2019) The Prion 2018 round tables (I): The structure of PrP(Sc). Prion 13:46–52

Benestad SL, Telling GC (2018) Chronic wasting disease: an evolving prion disease of cervids. Handb Clin Neurol 153:135–151

Benilova I, Reilly M, Terry C, Wenborn A, Schmidt C, Marinho AT, Risse E, Al Doujaily H, Wiggins DO, Sandberg MK, Wadsworth

JDF, Jat PS, Collinge J (2020) Highly infectious prions are not directly neurotoxic. Proc Natl Acad Sci USA 117:23815–23822
Bessen RA, Marsh RF (1994) Distinct PrP properties suggest the molecular basis of strain variation in transmissible mink encephalopathy. J Virol 68:7859–7868
Bolton DC, Bendheim PE (1991) Purification of scrapie agents: How far have we come. Curr Top Microbiol Immunol 172:39–55
Bolton DC, McKinley MP, Prusiner SB (1982) Identification of a protein that purifies with the scrapie prion. Science 218:1309–1311
Bruce ME, Will RG, Ironside JW, McConnell I, Drummond D, Suttie A, McCardle L, Chree A, Hope J, Birkett C, Cousens S, Fraser H, Bostock CJ (1997) Transmissions to mice indicate that "new variant" CJD is caused by the BSE agent. Nature 389:498–501
Cardone F, Liu QG, Petraroli R, Ladogana A, D'Alessandro M, Arpino C, Di Bari M, Macchi G, Pocchiari M (1999) Prion protein glycotype analysis in familial and sporadic Creutzfeldt-Jakob disease patients. Brain Res Bull 49:429–433
Chen SG, Parchi P, Brown P, Capellari S, Zou WQ, Cochran EJ, Vnencak-Jones CL, Julien J, Vital C, Mikol J, Lugaresi E, Autilio-Gambetti L, Gambetti P (1997) Allelic origin of the abnormal prion protein isoform in familial prion diseases. Nat Med 3:1009–1015
Choi JK, Cali I, Surewicz K, Kong Q, Gambetti P, Surewicz WK (2016) Amyloid fibrils from the N-terminal prion protein fragment are infectious. Proc Natl Acad Sci USA 113:13851–13856
Cobb NJ, Sonnichsen FD, McHaourab H, Surewicz WK (2007) Molecular architecture of human prion protein amyloid: a parallel, in-register beta-structure. Proc Natl Acad Sci USA 104:18946–18951
Collinge J (1999) Variant Creutzfeldt-Jakob disease. Lancet 354:317–323
Collinge J (2001) Prion diseases of humans and animals: their causes and molecular basis. Annu Rev Neurosci 24:519–550
Collinge J (2005) Molecular neurology of prion disease. J Neurol Neurosurg Psychiatry 76:906–919
Collinge J (2016) Mammalian prions and their wider relevance in neurodegenerative diseases. Nature 539:217–226
Collinge J, Clarke A (2007) A general model of prion strains and their pathogenicity. Science 318:930–936
Collinge J, Sidle KC, Meads J, Ironside J, Hill AF (1996) Molecular analysis of prion strain variation and the aetiology of "new variant" CJD. Nature 383:685–690
Cracco L, Xiao X, Nemani SK, Lavrich J, Cali I, Ghetti B, Notari S, Surewicz WK, Gambetti P (2019) Gerstmann-Straussler-Scheinker disease revisited: accumulation of covalently-linked multimers of internal prion protein fragments. Acta Neuropathol Commun 7:85
Dubochet J (2018) On the development of electron cryo-microscopy (Nobel Lecture). Angew Chem Int Ed Engl 57:10842–10846
Eisenberg DS, Sawaya MR (2017) Structural studies of amyloid proteins at the molecular level. Annu Rev Biochem 86:69–95
Escobar LE, Pritzkow S, Winter SN, Grear DA, Kirchgessner MS, Dominguez-Villegas E, Machado G, Townsend PA, Soto C (2020) The ecology of chronic wasting disease in wildlife. Biol Rev Camb Philos Soc 95:393–408
Falcon B, Zhang W, Murzin AG, Murshudov G, Garringer HJ, Vidal R, Crowther RA, Ghetti B, Scheres SHW, Goedert M (2018) Structures of filaments from Pick's disease reveal a novel tau protein fold. Nature 561:137–140
Falcon B, Zivanov J, Zhang W, Murzin AG, Garringer HJ, Vidal R, Crowther RA, Newell KL, Ghetti B, Goedert M, Scheres SHW (2019) Novel tau filament fold in chronic traumatic encephalopathy encloses hydrophobic molecules. Nature 568:420–423
Fitzpatrick AW, Saibil HR (2019) Cryo-EM of amyloid fibrils and cellular aggregates. Curr Opin Struct Biol 58:34–42
Fitzpatrick AWP, Falcon B, He S, Murzin AG, Murshudov G, Garringer HJ, Crowther RA, Ghetti B, Goedert M, Scheres SHW (2017) Cryo-EM structures of tau filaments from Alzheimer's disease. Nature 547:185–190
Fletcher CM, Harrison RA, Lachmann PJ, Neuhaus D (1994) Structure of a soluble, glycosylated form of the human complement regulatory protein CD59. Structure 2:185–199
Frank J (2018) Single-particle reconstruction of biological molecules-story in a sample (Nobel Lecture). Angew Chem Int Ed Engl 57:10826–10841
Furukawa H, Doh-ura K, Kikuchi H, Tateishi J, Iwaki T (1998) A comparative study of abnormal prion protein isoforms between Gerstmann-Sträussler-Scheinker syndrome and Creutzfeldt-Jakob disease. J Neurol Sci 158:71–75
Gabizon R, Telling G, Meiner Z, Halimi M, Kahana I, Prusiner SB (1996) Insoluble wild-type and protease-resistant mutant prion protein in brains of patients with inherited prion disease. Nat Med 2:59–64
Gallardo R, Ranson NA, Radford SE (2020) Amyloid structures: much more than just a cross-β fold. Curr Opin Struct Biol 60:7–16
Ghetti B, Piccardo P, Spillantini MG, Ichimiya Y, Porro M, Perini F, Kitamoto T, Tateishi J, Seiler C, Frangione B, Bugiani O, Giaccone G, Prelli F, Goedert M, Dlouhy SR, Tagliavini F (1996) Vascular variant of prion protein cerebral amyloidosis with t-positive neurofibrillary tangles: the phenotype of the stop codon 145 mutation in *PRNP*. Proc Natl Acad Sci USA 93:744–748
Ghetti B, Piccardo P, Zanusso G (2018) Dominantly inherited prion protein cerebral amyloidoses – a modern view of Gerstmann-Straussler-Scheinker. Handb Clin Neurol 153:243–269
Ghosh U, Thurber KR, Yau WM, Tycko R (2021) Molecular structure of a prevalent amyloid-β fibril polymorph from Alzheimer's disease brain tissue. Proc Natl Acad Sci USA 118:e2111863118. https://doi.org/10.1073/pnas.2111863118
Giaccone G, Verga L, Bugiani O, Frangione B, Serban D, Prusiner SB, Farlow MR, Ghetti B, Tagliavini F (1992) Prion protein preamyloid and amyloid deposits in Gerstmann-Straussler-Scheinker disease, Indiana kindred. Proc Natl Acad Sci USA 89:9349–9353
Glynn C, Sawaya MR, Ge P, Gallagher-Jones M, Short CW, Bowman R, Apostol M, Zhou ZH, Eisenberg DS, Rodriguez JA (2020) Cryo-EM structure of a human prion fibril with a hydrophobic, protease-resistant core. Nat Struct Mol Biol 27:417–423
Greenlee JJ, Greenlee MH (2015) The transmissible spongiform encephalopathies of livestock. ILAR J 56:7–25
Groveman BR, Dolan MA, Taubner LM, Kraus A, Wickner RB, Caughey B (2014) Parallel in-register intermolecular beta-sheet architectures for prion-seeded prion protein (PrP) amyloids. J Biol Chem 289:24129–24142
Hallinan GI, Ozcan KA, Hoq MR, Cracco L, Vago FS, Bharath SR, Li D, Jacobsen M, Doud EH, Mosley AL, Fernandez A, Garringer HJ, Jiang W, Ghetti B, Vidal R (2022) Cryo-EM structures of prion protein filaments from Gerstmann-Sträussler-Scheinker disease. Acta Neuropathol. https://doi.org/10.1007/s00401-022-02461-0
He S, Scheres SHW (2017) Helical reconstruction in RELION. J Struct Biol 198:163–176
Henderson R (2018) From electron crystallography to single particle cryoEM (Nobel Lecture). Angew Chem Int Ed Engl 57:10804–10825
Hill AF, Desbruslais M, Joiner S, Sidle KCL, Gowland I, Collinge J (1997) The same prion strain causes vCJD and BSE. Nature 389:448–450
Hill AF, Joiner S, Beck J, Campbell TA, Dickinson A, Poulter M, Wadsworth JD, Collinge J (2006) Distinct glycoform ratios of protease resistant prion protein associated with *PRNP* point mutations. Brain 129:676–685
Hill AF, Joiner S, Wadsworth JD, Sidle KC, Bell JE, Budka H, Ironside JW, Collinge J (2003) Molecular classification of sporadic Creutzfeldt-Jakob disease. Brain 126:1333–1346

Hoyt F, Standke HG, Artikis E, Schwartz CL, Hansen B, Li K, Hughson AG, Manca M, Thomas OR, Raymond GJ, Baron GS, Caughey B, Kraus A (2022) Cryo-EM structure of anchorless RML prion reveals variations in shared motifs between distinct strains. Nat Commun 13:4005. https://doi.org/10.1038/s41467-022-30458-6

Jo S, Kim T, Iyer VG, Im W (2008) CHARMM-GUI: a web-based graphical user interface for CHARMM. J Comput Chem 29:1859–1865

Kang HE, Bian J, Kane SJ, Kim S, Selwyn V, Crowell J, Bartz JC, Telling GC (2020) Incomplete glycosylation during prion infection unmasks a prion protein epitope that facilitates prion detection and strain discrimination. J Biol Chem 295:10420–10433

Katorcha E, Baskakov IV (2017) Analyses of N-linked glycans of PrPSc revealed predominantly 2,6-linked sialic acid residues. FEBS J 284:3727–3738

Kim MO, Takada LT, Wong K, Forner SA, Geschwind MD (2017) Genetic PrP prion diseases. Cold Spring Harb Perspect Biol 10:a033134. https://doi.org/10.1101/cshperspect.a033134

Kimanius D, Dong L, Sharov G, Nakane T, Scheres SHW (2021) New tools for automated cryo-EM single-particle analysis in RELION-4.0. Biochem J 478:4169–4185

Klohn P, Stoltze L, Flechsig E, Enari M, Weissmann C (2003) A quantitative, highly sensitive cell-based infectivity assay for mouse scrapie prions. Proc Natl Acad Sci USA 100:11666–11671

Kollmer M, Close W, Funk L, Rasmussen J, Bsoul A, Schierhorn A, Schmidt M, Sigurdson CJ, Jucker M, Fandrich M (2019) Cryo-EM structure and polymorphism of Abeta amyloid fibrils purified from Alzheimer's brain tissue. Nat Commun 10:4760

Kovacs GG, Ghetti B, Goedert M (2022) Classification of diseases with accumulation of Tau protein. Neuropathol Appl Neurobiol 48:e12792

Kovacs GG, Trabattoni G, Hainfellner JA, Ironside JW, Knight RS, Budka H (2002) Mutations of the prion protein gene phenotypic spectrum. J Neurol 249:1567–1582

Kraus A, Hoyt F, Schwartz CL, Hansen B, Artikis E, Hughson AG, Raymond GJ, Race B, Baron GS, Caughey B (2021) High-resolution structure and strain comparison of infectious mammalian prions. Mol Cell 81:4540–4551

Lövestam S, Scheres SHW (2022). High-throughput cryo-EM structure determination of amyloids. Preprint at bioRxiv 2022.02.07.479378. https://doi.org/10.1101/2022.02.07.479378.

Mahal SP, Baker CA, Demczyk CA, Smith EW, Julius C, Weissmann C (2007) Prion strain discrimination in cell culture: the cell panel assay. Proc Natl Acad Sci USA 104:20908–20913

Manka SW, Wenborn A, Betts J, Joiner S, Saibil HR, Wadsworth CJ, JDF. (2022a) A structural basis for prion strain diversity. Preprint at BioRxiv. https://doi.org/10.1101/2022.05.17.492259

Manka SW, Zhang W, Wenborn, A, Betts J, Joiner S, Saibil HR, Collinge J Wadsworth JDF. (2022b) 2.7 Å cryo-EM structure of *ex vivo* RML prion fibrils. Nat Commun 13:4004 https://doi.org/10.1038/s41467-022-30457-7

McKinley MP, Bolton DC, Prusiner SB (1983) A protease-resistant protein is a structural component of the scrapie prion. Cell 35:57–62

Mead S, Gandhi S, Beck J, Caine D, Gallujipali D, Carswell C, Hyare H, Joiner S, Ayling H, Lashley T, Linehan JM, Al Doujaily H, Sharps B, Revesz T, Sandberg MK, Reilly MM, Koltzenburg M, Forbes A, Rudge P, Brandner S, Warren JD, Wadsworth JD, Wood NW, Holton JL, Collinge J (2013) A novel prion disease associated with diarrhea and autonomic neuropathy. N Engl J Med 369:1904–1914

Mead S, Lloyd S, Collinge J (2019) Genetic factors in mammalian prion diseases. Annu Rev Genet 53:117–147

Mead S, Reilly MM (2015) A new prion disease: relationship with central and peripheral amyloidoses. Nat Rev Neurol 11:90–97

Meisl G, Kurt T, Condado-Morales I, Bett C, Sorce S, Nuvolone M, Michaels TCT, Heinzer D, Avar M, Cohen SIA, Hornemann S, Aguzzi A, Dobson CM, Sigurdson CJ, Knowles TPJ (2021) Scaling analysis reveals the mechanism and rates of prion replication *in vivo*. Nat Struct Mol Biol 28:365–372

Meyer RK, McKinley MP, Bowman K, Braunfeld MB, Barry RA, Prusiner SB (1986) Separation and properties of cellular and scrapie prion proteins. Proc Natl Acad Sci USA 83:2310–2314

Monaco S, Fiorini M, Farinazzo A, Ferrari S, Gelati M, Piccardo P, Zanusso G, Ghetti B (2012) Allelic origin of protease-sensitive and protease-resistant prion protein isoforms in Gerstmann-Straussler-Scheinker disease with the P102L mutation. PLoS ONE 7:e32382

Moreno JA, Telling GC (2017) Insights into mechanisms of transmission and pathogenesis from transgenic mouse models of prion diseases. Methods Mol Biol 1658:219–252

Moretto E, Stuart S, Surana S, Vargas JNS, Schiavo G (2022) The role of extracellular matrix components in the spreading of pathological protein aggregates. Front Cell Neurosci 16:844211

Pan KM, Baldwin MA, Nguyen J, Gasset M, Serban A, Groth D, Mehlhorn I, Huang Z, Fletterick RJ, Cohen FE, Prusiner SB (1993) Conversion of α-helices into β-sheets features in the formation of the scrapie prion proteins. Proc Natl Acad Sci USA 90:10962–10966

Parchi P, Chen SG, Brown P, Zou W, Capellari S, Budka H, Hainfellner J, Reyes PF, Golden GT, Hauw JJ, Gajdusek DC, Gambetti P (1998) Different patterns of truncated prion protein fragments correlate with distinct phenotypes in P102L Gerstmann-Sträussler-Scheinker disease. Proc Natl Acad Sci USA 95:8322–8327

Parchi P, Giese A, Capellari S, Brown P, Schulz-Schaeffer W, Windl O, Zerr I, Budka H, Kopp N, Piccardo P, Poser S, Rojiani A, Streichenberger N, Julien J, Vital C, Ghetti B, Gambetti P, Kretzschmar H (1999) Classification of sporadic Creutzfeldt-Jakob disease based on molecular and phenotypic analysis of 300 subjects. Ann Neurol 46:224–233

Pettersen EF, Goddard TD, Huang CC, Couch GS, Greenblatt DM, Meng EC, Ferrin TE (2004) UCSF Chimera–a visualization system for exploratory research and analysis. J Comput Chem 25:1605–1612

Piccardo P, Dlouhy SR, Lievens PMJ, Young K, Bird TD, Nochlin D, Dickson DW, Vinters HV, Zimmerman TR, Mackenzie IRA, Kish SJ, Ang LC, De Carli C, Pocchiari M, Brown P, Gibbs CJ, Gajdusek DC, Bugiani O, Ironside J, Tagliavini F, Ghetti B (1998) Phenotypic variability of Gerstmann-Straussler-Scheinker disease is associated with prion protein heterogeneity. J Neuropathol Exp Neurol 57:979–988

Piccardo P, Liepnieks JJ, William A, Dlouhy SR, Farlow MR, Young K, Nochlin D, Bird TD, Nixon RR, Ball MJ, DeCarli C, Bugiani O, Tagliavini F, Benson MD, Ghetti B (2001) Prion proteins with different conformations accumulate in Geustmann-Straussler-Scheinker disease caused by A117V and F198S mutations. Am J Pathol 158:2201–2207

Piccardo P, Manson JC, King D, Ghetti B, Barron RM (2007) Accumulation of prion protein in the brain that is not associated with transmissible disease. Proc Natl Acad Sci USA 104:4712–4717

Piccardo P, Seiler C, Dlouhy SR, Young K, Farlow MR, Prelli F, Frangione B, Bugiani O, Tagliavini F, Ghetti B (1996) Proteinase-K-resistant prion protein isoforms in Gerstmann- Straussler-Scheinker disease (Indiana kindred). J Neuropathol Exp Neurol 55:1157–1163

Priola SA, Chesebro B (1995) A single hamster PrP amino acid blocks conversion to protease- resistant PrP in scrapie-infected mouse neuroblastoma cells. J Virol 69:7754–7758

Prusiner SB (1998) Prions. Proc Natl Acad Sci USA 95:13363–13383

Prusiner SB, Bowman K, Groth DF (1987) Purification of scrapie prions. In: Prusiner SB, McKinley MP (eds) Prions: novel

Infectious pathogens causing scrapie and Creutzfeldt-Jakob disease. Academic Press, San Diego, pp 149–171
Prusiner SB, McKinley MP, Bowman K, Bolton DC, Bendheim PE, Groth DF, Glenner GG (1983) Scrapie prions aggregate to form amyloid-like birefringent rods. Cell 35:349–358
Rodriguez JA, Jiang L, Eisenberg DS (2017) Toward the atomic structure of PrP^{Sc}. Cold Spring Harb Perspect Biol 9:a031336. https://doi.org/10.1101/cshperspect.a031336
Safar J, Wille H, Itri V, Groth D, Serban H, Torchia M, Cohen FE, Prusiner SB (1998) Eight prion strains have PrP^{Sc} molecules with different conformations. Nat Med 4:1157–1165
Saibil HR (2022) Cryo-EM in molecular and cellular biology. Mol Cell 82:274–284
Salmona M, Morbin M, Massignan T, Colombo L, Mazzoleni G, Capobianco R, Diomede L, Thaler F, Mollica L, Musco G, Kourie JJ, Bugiani O, Sharma D, Inouye H, Kirschner DA, Forloni G, Tagliavini F (2003) Structural properties of Gerstmann-Straussler-Scheinker disease amyloid protein. J Biol Chem 278:48146–48153
Sandberg MK, Al Doujaily H, Sharps B, Clarke AR, Collinge J (2011) Prion propagation and toxicity in vivo occur in two distinct mechanistic phases. Nature 470:540–542
Sandberg MK, Al Doujaily H, Sharps B, De Oliveira MW, Schmidt C, Richard-Londt A, Lyall S, Linehan JM, Brandner S, Wadsworth JD, Clarke AR, Collinge J (2014) Prion neuropathology follows the accumulation of alternate prion protein isoforms after infective titre has peaked. Nat Commun 5:4347
Sawaya MR, Hughes MP, Rodriguez JA, Riek R, Eisenberg DS (2021) The expanding amyloid family: structure, stability, function, and pathogenesis. Cell 184:4857–4873
Scheres SHW (2020) Amyloid structure determination in RELION-3.1. Acta Crystallogr D Struct Biol 76:94–101
Schmidt C, Fizet J, Properzi F, Batchelor M, Sandberg MK, Edgeworth JA, Afran L, Ho S, Badhan A, Klier S, Linehan JM, Brandner S, Hosszu LL, Tattum MH, Jat P, Clarke AR, Klohn PC, Wadsworth JD, Jackson GS, Collinge J (2015) A systematic investigation of production of synthetic prions from recombinant prion protein. Open Biol 5:150165
Schweighauser M, Shi Y, Tarutani A, Kametani F, Murzin AG, Ghetti B, Matsubara T, Tomita T, Ando T, Hasegawa K, Murayama S, Yoshida M, Hasegawa M, Scheres SHW, Goedert M (2020) Structures of α-synuclein filaments from multiple system atrophy. Nature 585:464–469
Shi Y, Zhang W, Yang Y, Murzin AG, Falcon B, Kotecha A, van Beers M, Tarutani A, Kametani F, Garringer HJ, Vidal R, Hallinan GI, Lashley T, Saito Y, Murayama S, Yoshida M, Tanaka H, Kakita A, Ikeuchi T, Robinson AC, Mann DMA, Kovacs GG, Revesz T, Ghetti B, Hasegawa M, Goedert M, Scheres SHW (2021) Structure-based classification of tauopathies. Nature 598:359–363
Silvestrini MC, Cardone F, Maras B, Pucci P, Barra D, Brunori M, Pocchiari M (1997) Identification of the prion protein allotypes which accumulate in the brain of sporadic and familial Creutzfeldt-Jakob disease patients. Nat Med 3:521–525
Sonati T, Reimann RR, Falsig J, Baral PK, O'Connor T, Hornemann S, Yaganoglu S, Li B, Herrmann US, Wieland B, Swayampakula M, Rahman MH, Das D, Kav N, Riek R, Liberski PP, James MN, Aguzzi A (2013) The toxicity of antiprion antibodies is mediated by the flexible tail of the prion protein. Nature 501:102–106
Spagnolli G, Rigoli M, Orioli S, Sevillano AM, Faccioli P, Wille H, Biasini E, Requena JR (2019) Full atomistic model of prion structure and conversion. PLoS Pathog 15:e1007864
Stura EA, Muller BH, Bossus M, Michel S, Jolivet-Reynaud C, Ducancel F (2011) Crystal structure of human prostate-specific antigen in a sandwich antibody complex. J Mol Biol 414:530–544
Telling GC (2022) The shape of things to come: structural insights into how prion proteins encipher heritable information. Nat Commun 13:4003. https://doi.org/10.1038/s41467-022-31460-8
Telling GC, Parchi P, DeArmond SJ, Cortelli P, Montagna P, Gabizon R, Mastrianni J, Lugaresi E, Gambetti P, Prusiner SB (1996) Evidence for the conformation of the pathologic isoform of the prion protein enciphering and propagating prion diversity. Science 274:2079–2082
Terry C, Harniman RL, Sells J, Wenborn A, Joiner S, Saibil HR, Miles MJ, Collinge J, Wadsworth JDF (2019) Structural features distinguishing infectious *ex vivo* mammalian prions from non-infectious fibrillar assemblies generated *in vitro*. Sci Rep 9:376
Terry C, Wadsworth JDF (2019) Recent advances in understanding mammalian prion structure: a mini review. Front Mol Neurosci 12:169
Terry C, Wenborn A, Gros N, Sells J, Joiner S, Hosszu LL, Tattum MH, Panico S, Clare DK, Collinge J, Saibil HR, Wadsworth JD (2016) Ex vivo mammalian prions are formed of paired double helical prion protein fibrils. Open Biol 6:160035
Theint T, Nadaud PS, Aucoin D, Helmus JJ, Pondaven SP, Surewicz K, Surewicz WK, Jaroniec CP (2017) Species-dependent structural polymorphism of Y145Stop prion protein amyloid revealed by solid-state NMR spectroscopy. Nat Commun 8:753
Tranulis MA, Gavier-Widén D, Våge J, Nöremark M, Korpenfelt SL, Hautaniemi M, Pirisinu L, Nonno R, Benestad SL (2021) Chronic wasting disease in Europe: new strains on the horizon. Acta Vet Scand 63:48
Tycko R, Savtchenko R, Ostapchenko VG, Makarava N, Baskakov IV (2010) The α-helical C-terminal domain of full-length recombinant PrP converts to an in-register parallel β-sheet structure in PrP fibrils: evidence from solid state nuclear magnetic resonance. Biochemistry 49:9488–9497
Vazquez-Fernandez E, Vos MR, Afanasyev P, Cebey L, Sevillano AM, Vidal E, Rosa I, Renault L, Ramos A, Peters PJ, Fernandez JJ, van Heel M, Young HS, Requena JR, Wille H (2016) The structural architecture of an infectious mammalian prion using electron cryomicroscopy. PLoS Pathog 12:e1005835
Wadsworth JD, Asante EA, Collinge J (2010) Contribution of transgenic models to understanding human prion disease. Neuropathol Appl Neurobiol 36:576–597
Wadsworth JD, Asante EA, Desbruslais M, Linehan J, Joiner S, Gowland I, Welch J, Stone L, Lloyd S, Hill AF, Brandner S, Collinge J (2004) Human prion protein with valine 129 prevents expression of variant CJD phenotype. Science 306:1793–1796
Wadsworth JD, Collinge J (2011) Molecular pathology of human prion disease. Acta Neuropathol 121:69–77
Wadsworth JD, Joiner S, Linehan J, Cooper S, Powell C, Mallinson G, Buckell J, Gowland I, Asante EA, Budka H, Brandner S, Collinge J (2006) Phenotypic heterogeneity in inherited prion disease (P102L) is associated with differential propagation of protease-resistant wild-type and mutant prion protein. Brain 129:1557–1569
Wang LQ, Zhao K, Yuan HY, Li XN, Dang HB, Ma Y, Wang Q, Wang C, Sun Y, Chen J, Li D, Zhang D, Yin P, Liu C, Liang Y (2021) Genetic prion disease-related mutation E196K displays a novel amyloid fibril structure revealed by cryo-EM. Sci Adv 7:eabg9676
Wang LQ, Zhao K, Yuan HY, Wang Q, Guan Z, Tao J, Li XN, Sun Y, Yi CW, Chen J, Li D, Zhang D, Yin P, Liu C, Liang Y (2020) Cryo-EM structure of an amyloid fibril formed by full-length human prion protein. Nat Struct Mol Biol 27:598–602
Watson N, Brandel JP, Green A, Hermann P, Ladogana A, Lindsay T, Mackenzie J, Pocchiari M, Smith C, Zerr I, Pal S (2021) The importance of ongoing international surveillance for Creutzfeldt-Jakob disease. Nat Rev Neurol 17:362–379

Webb TE, Poulter M, Beck J, Uphill J, Adamson G, Campbell T, Linehan J, Powell C, Brandner S, Pal S, Siddique D, Wadsworth JD, Joiner S, Alner K, Petersen C, Hampson S, Rhymes C, Treacy C, Storey E, Geschwind MD, Nemeth AH, Wroe S, Collinge J, Mead S (2008) Phenotypic heterogeneity and genetic modification of P102L inherited prion disease in an international series. Brain 131:2632–2646

Wenborn A, Terry C, Gros N, Joiner S, D'Castro L, Panico S, Sells J, Cronier S, Linehan JM, Brandner S, Saibil HR, Collinge J, Wadsworth JD (2015) A novel and rapid method for obtaining high titre intact prion strains from mammalian brain. Sci Rep 5:10062

Will RG, Ironside JW, Zeidler M, Cousens SN, Estibeiro K, Alperovitch A, Poser S, Pocchiari M, Hofman A, Smith PG (1996) A new variant of Creutzfeldt-Jakob disease in the UK. Lancet 347:921–925

Wuthrich K, Riek R (2001) Three-dimensional structures of prion proteins. Adv Protein Chem 57:55–82

Yang Y, Arseni D, Zhang W, Huang M, Lövestam S, Schweighauser M, Kotecha A, Murzin AG, Peak-Chew SY, MacDonald J, Lavenir I, Garringer HJ, Gelpi E, Newell KL, Kovacs GG, Vidal R, Ghetti B, Ryskeldi-Falcon B, Scheres SHW, Goedert M (2022a) Cryo-EM structures of amyloid-β 42 filaments from human brains. Science 375:167–172

Yang Y, Shi Y, Schweighauser M, Zhang X, Kotecha A, Murzin AG, Garringer HJ, Cullinane PW, Saito Y, Foroud T, Warner TT, Hasegawa K, Vidal R, Murayama S, Revesz T, Ghetti B, Hasegawa M, Lashley T, Scheres SHW, Goedert M (2022b) Cryo-EM structures of α-synuclein filaments from Parkinson's disease and dementia with Lewy bodies. Preprint at BioRxiv. https://doi.org/10.1101/2022.07.12.499706

Zhang W, Tarutani A, Newell KL, Murzin AG, Matsubara T, Falcon B, Vidal R, Garringer HJ, Shi Y, Ikeuchi T, Murayama S, Ghetti B, Hasegawa M, Goedert M, Scheres SHW (2020) Novel tau filament fold in corticobasal degeneration. Nature 580:283–287

Zivanov J, Nakane T, Forsberg BO, Kimanius D, Hagen WJ, Lindahl E, Scheres SH (2018) New tools for automated high-resolution cryo-EM structure determination in RELION-3. Elife 7:e42166